Relativistic disks as sources of static vacuum spacetimes

Jiří Bičák,* D. Lynden-Bell, and Joseph Katz†
Institute of Astronomy, The Observatories, Cambridge CB3 0HA, United Kingdom
(Received 19 October 1992)

Among known finite-mass nonspherical solutions of Einstein's equations few have physical sources. We show that most vacuum Weyl solutions can arise as the metrics of counter-rotating relativistic disks. We give the metric for the general counter-rotating relativistic disk and show how the Curzon, Schwarzschild, Zipoy-Vorhees, and Israel-Kahn metrics can be generated by the disks. The physical properties of the disks are discussed and illustrated. The central gravitational redshift can become arbitrarily large. The disks with new metrics are discussed elsewhere.

PACS number(s): 04.20.Jb

I. INTRODUCTION

Kuzmin [1] gave a clever way of finding the Newtonian gravity field of a disk. He imagined a point mass placed at a distance b below the center $R=0$ of a plane $z=0$. Above the plane this gives a solution of Laplace's equation $\nabla^2\nu=0$. Kuzmin then imagined the potential ν obtained by reflecting this $z\geq 0$ potential in $z=0$ so as to give a symmetrical solution of Laplace's equation both above and below the plane. This is continuous, but has a discontinuous normal derivative on $z=0$. By Poisson's equation the jump in the normal derivative gives a surface density of mass on the plane. In Kuzmin's case it gives

$$\nu=-GM/r_b \ , \tag{1.1}$$

where

$$r_b^2=R^2+(|z|+b)^2 \ .$$

So $[\partial\nu/\partial z]_{0-}^{0+}=2GMb/(R^2+b^2)^{3/2}$ and the corresponding classical surface density of mass is

$$\Sigma(R)=(2\pi)^{-1}Mb/(R^2+b^2)^{3/2} \ . \tag{1.2}$$

The total mass of the disk is M, and R is the cylindrical polar coordinate; in the relativistic literature, this is sometimes called ρ.

Recently, Evans and de Zeeuw [2] have shown that any axially symmetrical disk can be analyzed into a superposition of Kuzmin disks of different b and with different weights $W(b)$. Their notation differs from ours since they did not use Kuzmin's picture of a mass below the disk. Employing this picture, we see that a general axially symmetrical disk has a gravitational potential above its plane equal to that of a line distribution of mass (positive or negative) below the plane. Thus the general classical disk has a potential

$$\nu=-G\int\frac{W(b)db}{[R^2+(|z|+b)^2]^{1/2}} \tag{1.3}$$

and a surface density on the disk,

$$\Sigma(R)=(2\pi)^{-1}\int\frac{W(b)b\,db}{(R^2+b^2)^{3/2}} \ . \tag{1.4}$$

The total mass is $\int W(b)db$.

For Kuzmin's disk, W is a δ function and in general W is a distribution rather than a continuous function. Weyl [3] has shown that solutions of Laplace's equation may be used to generate axially symmetrical solutions in general relativity. In the particular case when the stress tensor satisfies $T_R^R+T_z^z=0$, Weyl's metric takes the form (hereafter the velocity of light, $c=1$)

$$ds^2=-e^{2\nu}dt^2+e^{2(\zeta-\nu)}(dR^2+dz^2)+R^2e^{-2\nu}d\phi^2 \ , \tag{1.5}$$

and away from matter ν satisfies Laplace's equation with ∇^2 the normal axially symmetrical operator of flat space,

$$\nabla^2\nu=\frac{1}{R}\frac{\partial}{\partial R}\left[R\frac{\partial\nu}{\partial R}\right]+\frac{\partial^2\nu}{\partial z^2}=0 \ . \tag{1.6}$$

Thus classical solutions can be used to generate relativistic ones; however, the relationship between the jump in the gradient of ν across the plane and the surface density is not the classical one. Furthermore, a rotating disk gives a dragging of inertial frames and so does not generate a metric of Weyl's type. To avoid that problem, we take our disks to be made of two equal streams of collisionless particles (stars) that circulate in opposite directions around the disk's center. Following Morgan and Morgan [4], we refer to these as counter-rotating disks. If σ_p is the surface-proper rest mass density of *one* stream, measured in axes that move with it, then the surface density of its *rest* mass in our fixed static axes is $\frac{1}{2}\sigma_0=\sigma_p(1-V^2)^{-1/2}$, where V is the velocity of the stream. The surface energy density of the *pair* of streams in fixed axes is

$$-\tau_t^t=\sigma=\sigma_0/(1-V^2)^{1/2}=2\sigma_p/(1-V^2) \ , \tag{1.7}$$

and the tangential pressure caused by the counter rotation is

---

*Permanent address: Department of Theoretical Physics, Charles University, 18000 Prague 8, Czech Republic.

†Permanent address: Racah Institute of Physics, Hebrew University, Jerusalem 91904, Israel.

$$\tau_\phi^\phi = 2\sigma_p V^2/(1-V^2) = \sigma V^2 \ . \tag{1.8}$$

In our disks σ, σ_p, and V are all functions of R. Morgan and Morgan [4] gave explicitly the solution for a uniformly counter-rotating disk, while Lynden-Bell and Pineault [5] gave solutions in which V is constant and the disk has a finite radius a. When in the above disks a approaches infinity, their metric takes the pretty form

$$\begin{aligned} ds^2 = &-\left[r\cos^2\frac{\theta}{2}\right]^{2N} dt^2 \\ &+\left[r\cos^2\frac{\theta}{2}\right]^{-2N} \cos^{8N^2}\frac{\theta}{2}(dr^2+r^2d\theta^2) \\ &+\left[r\cos^2\frac{\theta}{2}\right]^{-2N} r^2\sin^2\theta\, d\phi^2 \ , \end{aligned} \tag{1.9}$$

where $N=V^2/(1+V^2)$ and $\theta \le \pi/2$. Below the disk, θ is replaced by $-\theta$. They also discussed self-similar truly rotating disks with frame dragging [6].

The metric (1.9), without being interpreted as the metric of the counter-rotating disk, was obtained by Godfrey [7]; he found all Weyl metrics admitting homothetic motion.

Katz pointed out that when $V=1$ the metric (1.9) reduces to the Rindler metric of flat space as seen by an observer accelerating uniformly toward the disk. Lemos [8] gave these transformations and used them to find the geodesics in this metric.

When we use Kuzmin's idea in Weyl's coordinates to generate a relativistic disk, we find that the metric above the disk is that of a point in Weyl's coordinates, i.e., the Curzon metric [9]. We shall refer to the resulting disks as the Kuzmin-Curzon disks [10]. These are our natural building blocks. We work out their details in Sec. III.

We also consider the disk that is obtained by putting the source of Weyl's form of the Schwarzschild solution below the disk. This corresponds to taking $W(b)$ to be a uniform rod of length $2m$ and weight $\frac{1}{2}$. A sequence of different disks is obtained by centering the rod of length $b-a>0$ at a distance $\frac{1}{2}(a+b)$ below the disk. Another way of arriving at this same metric is to subtract the potentials of two infinite counter-rotating $V=1$ disks at distances a and b below the center. Thus there are remarkable relationships between the infinite disks of Lynden-Bell and Pineault and the Schwarzschild disks. For the Schwarzschild disks, the line mass density has to be $\frac{1}{2}$. By taking uniform finite lengths of other line densities, we generate disks corresponding to the Zipoy-Voorhees solution [11]. Indeed, the general infinite Lynden-Bell and Pineault solutions with $V<1$ may be obtained from those by taking the upper end of the uniform line density to touch the disk and sending the lower end off to infinity.

Classical potentials are linear, and so disks can be superposed linearly. This is not true in relativity in general, but as we solve $\nabla^2\nu=0$ to find ν, we may superpose solutions for ν. The equations defining the function ζ in (1.5) are quadratic in ν, and so there is no straightforward superposition principle for ζ. Nevertheless, we are able to give a general formula for the ζ derived from a general weight function $W(b)$. This allows us to give the general solution for a disk of any weight function W. This general solution obviously involves integrals over the weight function, which has to be specified before the integrations are carried out. When W is a sum of n δ functions, we find the disk whose metric corresponds to n collinear Curzon singularities below the disk. Related metrics in the absence of a disk were considered by Israel and Kahn [12].

II. RELATIVISTIC DISKS: THE GENERAL SOLUTION

Following Synge [3], Einstein's field equations, when the metric is (1.5), become

$$\nabla^2\nu = 4\pi G\exp[2(\zeta-\nu)](T_\phi^\phi - T_t^t) \ , \tag{2.1}$$

$$\frac{\partial\zeta}{\partial R} = R\left[\left[\frac{\partial\nu}{\partial R}\right]^2 - \left[\frac{\partial\nu}{\partial z}\right]^2\right] , \tag{2.2}$$

$$\frac{\partial\zeta}{\partial z} = 2R\frac{\partial\nu}{\partial R}\frac{\partial\nu}{\partial z} \ , \tag{2.3}$$

$$\frac{\partial^2\zeta}{\partial R^2} + \frac{\partial^2\zeta}{\partial z^2} - \nabla^2\nu + \left[\frac{\partial\nu}{\partial R}\right]^2 + \left[\frac{\partial\nu}{\partial z}\right]^2 = 4\pi G e^{2(\zeta-\nu)}(T_t^t + T_\phi^\phi) \ , \tag{2.4}$$

where ∇^2 is the operator of (1.6). Away from matter, (2.1) reduces to Laplace's equation. So by choosing its right-hand side in the form $4\pi G S(R)\delta(z)$ the problem reduces to the classical potential problem. The stress energy tensor when integrated through the disk gives the surface stress tensor of the disk itself:

$$\tau_\phi^\phi = \int T_\phi^\phi e^{\zeta-\nu} dz = \sigma V^2 \ , \tag{2.5}$$

$$\tau_t^t = \int T_t^t e^{\zeta-\nu} dz = -\sigma \ . \tag{2.6}$$

Using (2.1) in (2.4) and integrating through the disk, we find

$$\left[\frac{\partial\zeta}{\partial z}\right]_{0-}^{0+} = 8\pi G e^{\zeta-\nu}\tau_\phi^\phi = 8\pi G\sigma e^{\zeta-\nu}V^2 \tag{2.7}$$

and, from (2.1),

$$\left[\frac{\partial\nu}{\partial z}\right]_{0-}^{0+} = 4\pi G e^{\zeta-\nu}(\tau_\phi^\phi - \tau_t^t) = 4\pi G\sigma e^{\zeta-\nu}(1+V^2) \ . \tag{2.8}$$

Similarly, integrating (2.3),

$$\left[\frac{\partial\zeta}{\partial z}\right]_{0-}^{0+} = 2R\frac{\partial\nu}{\partial R}\left[\frac{\partial\nu}{\partial z}\right]_{0-}^{0+} \ . \tag{2.9}$$

Hence, finally,

$$R\frac{\partial\nu}{\partial R} = \tau_\phi^\phi/(\tau_\phi^\phi - \tau_t^t) = V^2/(1+V^2) \ . \tag{2.10}$$

In practice, the total energy within R is given by $\int_0^R 2\pi\sigma e^{\zeta-\nu}e^{-\nu}R\,dR$, and so it is $\sigma e^{\zeta-\nu}$ that we need rather than σ itself. Equations (2.10) and (2.8) are thus sufficient for calculations of disk structure even without the determination of ζ. Nevertheless, we do not get the complete metric until ζ is determined; so we shall now attack that problem initially following Ernst's method.

We write

$$D=\frac{\partial}{\partial R}-i\frac{\partial}{\partial z} . \tag{2.11}$$

This operator remains the same if $z+b$ is written for z.

If we center spherical polar coordinates anywhere on the axis and write

$$D_\theta=\frac{\partial}{\partial \theta}-ir\frac{\partial}{\partial r} , \tag{2.12}$$

then

$$D=r^{-1}e^{i\theta}D_\theta . \tag{2.13}$$

Equations (2.2) and (2.3), combined in the form

$$D\zeta=R(D\nu)^2 , \tag{2.14}$$

may be rewritten

$$D_\theta\zeta=\sin\theta e^{i\theta}(D_\theta\nu)^2 . \tag{2.15}$$

For the Kuzmin-Curzon disk, $\nu=-GM/r_b$ above the disk, where r_b is measured from a point on the axis at a distance b below the disk. Hence, centering our spherical polars there, (2.15) reduces to

$$\frac{\partial\zeta}{\partial\theta}-ir_b\frac{\partial\zeta}{\partial r_b}=-\sin\theta e^{i\theta}r_b^2G^2M^2/r_b^4 ,$$

$$\sin\theta=R/r_b . \tag{2.16}$$

Taking the real part and integrating from r_b to ∞, we get

$$\zeta=-\tfrac{1}{2}G^2M^2R^2/r_b^4 , \tag{2.17}$$

where we have used the boundary condition that $\zeta\to 0$ at infinity. The θ integration gives the same result as it must since $\nabla^2\nu=0$ ensures that (2.2) and (2.3) are consistent.

Although this technique works for the Kuzmin-Curzon family of relativistic disks and yields, of course, the Curzon metric, it does not work simply in the general case. If ν_a and ν_b are two solutions of Laplace's equations and if the corresponding ζ's are ζ_a and ζ_b, then the ζ corresponding to $\nu_a+\nu_b$ will not be $\zeta_a+\zeta_b$ because (2.2) and (2.3) are quadratic rather than linear. In practice, we may write $\zeta=\zeta_a+\zeta_b+2\zeta_{ab}$, where, by subtraction of the known solutions, (2.2) and (2.3) become

$$\frac{\partial\zeta_{ab}}{\partial R}=R\left[\frac{\partial\nu_a}{\partial R}\frac{\partial\nu_b}{\partial R}-\frac{\partial\nu_a}{\partial z}\frac{\partial\nu_b}{\partial z}\right] , \tag{2.18}$$

$$\frac{\partial\zeta_{ab}}{\partial z}=R\left[\frac{\partial\nu_a}{\partial R}\frac{\partial\nu_b}{\partial z}+\frac{\partial\nu_a}{\partial z}\frac{\partial\nu_b}{\partial R}\right] . \tag{2.19}$$

These equations are automatically consistent because the corresponding equations for ζ_a and ζ_b were. When $\nu_a=\nu_b$, Eqs. (2.18) and (2.19) become (2.2) and (2.3). In the general case, we have

$$\nu=-G\int\frac{W(b)db}{[R^2+(|z|+b)^2]^{1/2}} . \tag{2.20}$$

Because (2.2) and (2.3) are quadratic in ν, the general ζ can be expressed as an integral over pairs of individual contributions to ν. Thus ζ takes the form

$$\zeta=G^2\int\int W(b_1)W(b_2)Z_1(b_1,b_2,\mathbf{r})db_1db_2 , \tag{2.21}$$

where Z arises as the cross term between the elementary potentials ν_1 and ν_2:

$$\nu_i=[R^2+(|z|+b_i)^2]^{-1/2}=1/r_i \quad \text{for } z>0 . \tag{2.22}$$

Equations (2.18) and (2.19) will be true when ζ_{ab} is replaced by Z and ν_a,ν_b are replaced by ν_1 and ν_2. Again, the cross terms inherit their consistency from that of the constituents ν_1 and ν_2. Using (2.11), Eqs. (2.18) and (2.19) become

$$DZ\,D(\ln R)=D\nu_1D\nu_2 . \tag{2.23}$$

We now transform to spheroidal coordinates based on the foci $R=0$, $z=-b_1, -b_2$. To do this we write

$$z+\bar{b}+iR=\tfrac{1}{2}\Delta\cosh(\xi_1+i\xi_2) , \tag{2.24}$$

with $\Delta=b_2-b_1$ and $2\bar{b}=b_1+b_2$.

Defining $\lambda=\cosh\xi_1$ and $\mu=\cos\xi_2$, we find

$$2(z+\bar{b})=\Delta\lambda\mu , \tag{2.25}$$

$$2R=\Delta[(\lambda^2-1)(1-\mu^2)]^{1/2} . \tag{2.26}$$

The operator D becomes

$$D=\frac{\partial(\xi_1+i\xi_2)}{i\partial(R-iz)}\left[\frac{\partial}{\partial\xi_1}+i\frac{\partial}{\partial\xi_2}\right] , \tag{2.27}$$

but, by (2.25),

$$\frac{\partial}{\partial\xi_1}=(\lambda^2-1)^{1/2}\frac{\partial}{\partial\lambda} , \quad \frac{\partial}{\partial\xi_2}=(1-\mu^2)^{1/2}\frac{\partial}{\partial\mu} , \tag{2.28}$$

and so (2.23) becomes

$$D_*Z\,D_*(\ln R)=D_*\nu_1D_*\nu_2 , \tag{2.29}$$

where

$$D_*=(\lambda^2-1)^{1/2}\frac{\partial}{\partial\lambda}+i(1-\mu^2)^{1/2}\frac{\partial}{\partial\mu} . \tag{2.30}$$

Furthermore, we have

$$r_1=[R^2+(z+b_1)^2]^{1/2}=\frac{\Delta}{2}(\lambda-\mu) ,$$

$$z\geq 0 . \tag{2.31}$$

$$r_2=[R^2+(z+b_2)^2]^{1/2}=\frac{\Delta}{2}(\lambda+\mu) ,$$

From the real and imaginary parts of (2.29), we eliminate $\partial Z/\partial\mu$ and deduce that

$$\frac{\Delta^2}{4}\frac{\partial Z}{\partial\lambda}=\frac{(1-\mu^2)\lambda}{(\lambda^2-\mu^2)^2} . \tag{2.32}$$

Using the boundary condition that $Z \to 0$ at infinity where space is flat, we have

$$Z = -\frac{2}{\Delta^2}\frac{(1-\mu^2)}{(\lambda^2-\mu^2)} = -\frac{1}{2r_1 r_2}\left[1-\left[\frac{r_2-r_1}{b_2-b_1}\right]^2\right] . \tag{2.33}$$

Putting this into (2.21), we find

$$\zeta = -\frac{G^2}{2}\int\int \frac{W(b_1)W(b_2)}{r_1 r_2}\left[1-\left[\frac{r_2-r_1}{b_2-b_1}\right]^2\right] db_1 db_2 . \tag{2.34}$$

This is our formal solution for ζ.

However, the integrations look awkward because r_1 and r_2 depend on b_1 and b_2 via (2.31). In practice, (2.34) may be simplified by using the variables ϕ_1, ϕ_2, where

$$b_i + |z| = R \sinh\phi_i , \quad i = 1,2 . \tag{2.35}$$

Then

$$r_i = R \cosh\phi_i , \quad db_i = R \cosh\phi_i d\phi_i . \tag{2.36}$$

Thus,

$$\zeta = \tfrac{1}{2}G^2 \int\int W_1 W_2 \left[\left[\frac{\cosh\phi_2 - \cosh\phi_1}{\sinh\phi_2 - \sinh\phi_1}\right]^2 - 1\right] d\phi_1 d\phi_2 . \tag{2.37}$$

Finally, putting $u_i = e^{\phi_i}$, we have

$$\zeta = -2G^2 \int\int \frac{W_1 W_2}{(u_1 u_2 + 1)^2} du_1 du_2 , \tag{2.38}$$

where

$$W_i = W\left[\tfrac{1}{2}R\left[u_i - \frac{1}{u_i}\right] - |z|\right] , \quad i = 1,2 . \tag{2.39}$$

The upper and lower limits of integration are given by

$$u_{\max} = (b_{\max} + |z| + r_{\max})/R , \tag{2.40}$$

where

$$r_{\max}^2 = R^2 + (|z| + b_{\max})^2 , \tag{2.41}$$

and similar equations with min written for max.

In the special case in which $W = \text{const} = N$ between $b_{\min}$ and $b_{\max}$, the integral is readily evaluated and gives

$$\zeta = -2N^2 G^2 \ln\left|\frac{(u_{\max}^2+1)(u_{\min}^2+1)}{(u_{\max}u_{\min}+1)^2}\right| . \tag{2.42}$$

After some manipulation this may be put in the form

$$\zeta = 2G^2 N^2 \ln\left|\frac{(r_{\max}+r_{\min})^2 - (b_{\max}-b_{\min})^2}{4 r_{\max} r_{\min}}\right| , \tag{2.43}$$

where $r_{\max}, r_{\min}$ are given by (2.41). The potential ν, given by (2.20), is

$$\begin{aligned}\nu &= GN \ln\left|\frac{r_{\min}+|z|+b_{\min}}{r_{\max}+|z|+b_{\max}}\right| \\ &= GN \ln\left|\frac{r_{\max}+r_{\min}-(b_{\max}-b_{\min})}{r_{\max}+r_{\min}+(b_{\max}-b_{\min})}\right| .\end{aligned} \tag{2.44}$$

The pair (2.43) and (2.44) represents the Zipoy-Voorhees metrics [11]; with $N = \frac{1}{2}$, these go over into the Schwarzschild metric with $GM = \frac{1}{2}(b_{\max} - b_{\min})$. When $W(b)$ is a sum of δ functions of weights w_i at $z = -b_i$, $i = 1, \ldots, p$, then we see at once from (2.20) and (2.34) that

$$\begin{aligned}\nu &= -G\sum_{i=1}^{p}\frac{w_i}{r_i} , \\ \zeta &= -\tfrac{1}{2}G^2 \sum_{i=1}^{p}\sum_{j=1}^{p}\frac{w_i w_j}{r_i r_j}\left[1-\left[\frac{r_i-r_j}{b_i-b_j}\right]^2\right] .\end{aligned} \tag{2.45}$$

Somewhat similar solutions with Schwarzschild rods were analyzed by Israel and Kahn [12]. Bonnor and Swaminarayan [13] discussed four Curzon particles and Bičák, Hoenselaers, and Schmidt [14] the point particles with arbitrary multipole structure.

III. PROPERTIES OF THE DISKS

In classical galactic dynamics, the following quantities are commonly used to characterize the axisymmetric disks: first, the gravitational potential $\nu(R,z)$; second, the circular velocity v with which stars orbit around the center ("the rotation curve"),

$$v(R) = \left[R\frac{\partial \nu}{\partial R}\right]^{1/2} , \tag{3.1}$$

with the corresponding angular velocity being

$$\omega = v/R ; \tag{3.2}$$

next, the distribution of the specific angular momentum of stars in circular orbits in the disk, which, in the classical case, is simply given by

$$j(R) = Rv ; \tag{3.3}$$

and, finally, the classical surface mass density as determined by the jump in the normal derivative of the potential:

$$\Sigma(R) = (4\pi G)^{-1}\left[\frac{\partial \nu}{\partial z}\right]_{0-}^{0+} . \tag{3.4}$$

In the case of our relativistic disks, the magnitude of the velocity of counter-rotating streams, as measured by the local static observers, follows from (2.10):

$$V = \left[\frac{R(\partial\nu/\partial R)}{1-R(\partial\nu/\partial R)}\right]^{1/2} . \tag{3.5}$$

The angular velocity of the counter rotation, as measured by observers at infinity, $\Omega = d\varphi/dt$, is given by

$$\Omega = Ve^{2\nu}/R . \tag{3.6}$$

The specific angular momentum of a particle with rest mass μ rotating at radius R, defined as $h=(p_\varphi/\mu)=g_{\varphi\varphi}d\varphi/d\tau$ (τ particle's proper time), can be written in the form

$$h=RVe^{-\nu}/(1-V^2)^{1/2}\ , \tag{3.7}$$

where V is given by (3.5). Finally, the surface mass-energy density σ and the surface rest mass density σ_0 follow from (2.8) and (3.5):

$$\sigma(R)=(4\pi G)^{-1}\left[\frac{\partial\nu}{\partial z}\right]_{0-}^{0+}e^{\nu-\zeta}\left[1-R\frac{\partial\nu}{\partial R}\right]\ , \tag{3.8}$$

$$\sigma_0(R)=(4\pi G)^{-1}\left[\frac{\partial\nu}{\partial z}\right]_{0-}^{0+}\times e^{\nu-\zeta}\left[\left[1-2R\frac{\partial\nu}{\partial R}\right]\left[1-R\frac{\partial\nu}{\partial R}\right]\right]^{1/2}\ . \tag{3.9}$$

Another quantity of interest in static spacetimes is the redshift z of a photon emitted by an atom at rest and received by a static observer at infinity. The redshift factor $1+z$ (no confusion with coordinate z) is given by

$$1+z=(|g_{00}|)^{-1/2}=e^{-\nu}\ . \tag{3.10}$$

We shall now discuss these quantities for the Kuzmin-Curzon disk and for the generalized Schwarzschild disks.

A. Kuzmin-Curzon disk

The classical Kuzmin disk has a potential ν given by (1.1) and a density Σ by (1.2). Other quantities of interest such as the velocity of the rotating flow v and its angular velocity ω take a particularly simple form in terms of the dimensionless mass parameter

$$\frac{GM}{b}\equiv N \tag{3.11}$$

and a radial parameter β in the range [0,1],

$$\beta=\frac{b}{(b^2+R^2)^{1/2}}\ ; \tag{3.12}$$

$\beta=0$ for $R=\infty$, $\beta=1$ for $R=0$. In this notation the classical density is

$$\Sigma=\frac{N}{2\pi Gb}\beta^3\ . \tag{3.13}$$

The circular velocity given by

$$v^2=N\beta(1-\beta^2) \tag{3.14}$$

and the corresponding angular velocity

$$\omega=\frac{1}{b}(N\beta^3)^{1/2}\ . \tag{3.15}$$

The relativistic Kuzmin-Curzon disk is described by two functions: the potential ν and the function ζ given in (2.17). It is useful to have them side by side:

$$\nu=-\frac{GM}{r_b}\ ,\quad \zeta=-\frac{1}{2}\left[\frac{GMR}{r_b^2}\right]^2\ ,\quad r_b^2=R^2+(b+|z|)^2\ . \tag{3.16}$$

Their value on the disk is

$$\nu_D=-N\beta\ ,\quad \zeta_D=-\tfrac{1}{2}N^2\beta^2(1-\beta^2)\ . \tag{3.17}$$

The energy tensor components of the disk τ_t^t and τ_ϕ^ϕ, as given by (2.7) and (2.8), are here

$$-\tau_t^t=\sigma=\frac{N}{2\pi Gb}\beta^3[1-N\beta(1-\beta^2)]e^{\nu_D-\zeta_D}\ , \tag{3.18}$$

$$\tau_\phi^\phi=\sigma V^2=\frac{N^2}{2\pi Gb}\beta^4(1-\beta^2)e^{\nu_D-\zeta_D}\ , \tag{3.19}$$

where V is the relativistic velocity (3.5).

Since $V^2\le 1$, we must have

$$\frac{\tau_\phi^\phi}{-\tau_t^t}=V^2=\frac{N\beta(1-\beta^2)}{1-N\beta(1-\beta^2)}=\frac{v^2}{1-v^2}\le 1\ . \tag{3.20}$$

Equation (3.20) must hold for any value of β, that is, at any radial distance. The maximum of V^2 occurs at

$$\beta^2=\tfrac{1}{3}\quad\text{or}\quad R=\sqrt{2}b\ . \tag{3.21}$$

Its value is smaller than 1 if

$$N=\frac{GM}{b}\le\frac{3\sqrt{3}}{4}\simeq 1.30\ . \tag{3.22}$$

The condition (3.20) that the velocity of the counter-rotating streams does not exceed the velocity of light reduces to the dominant energy condition [15]. If the disk is made of some material more exotic than the streams, satisfying, however, the weak-energy condition, i.e.,

$$-\tau_t^t\ge 0\quad\text{or}\quad 1-N\beta(1-\beta^2)\ge 0\ , \tag{3.23}$$

a bigger mass parameter would be admissible:

$$N=\frac{GM}{b}\le\frac{3\sqrt{3}}{2}\simeq 2.6\ . \tag{3.24}$$

The angular velocity of counter rotation [Eq. (3.6)] takes the form

$$\Omega=\omega e^{-2N\beta}[1-N\beta(1-\beta^2)]^{-1/2}\ , \tag{3.25}$$

with ω being the corresponding classical angular velocity (3.2), and the specific angular momentum (3.7) reads

$$h/b=(N/\beta)^{1/2}(1-\beta^2)e^{N\beta}[1-2N\beta(1-\beta^2)]^{-1/2}\ . \tag{3.26}$$

The classical specific angular momentum

$$j/b=(N/\beta)^{1/2}(1-\beta^2) \tag{3.27}$$

is an increasing function of R, and as $R\to\infty\,(\beta\to 0)$, $h/b\simeq j/b\propto\beta^{-1/2}$. The behavior of h/b closer to the central regions is more complicated. [See Fig. 1(b) and below.]

For the surface mass and rest mass densities (3.8) and (3.9), we now obtain

$$\sigma=(N\beta^3/2\pi Gb)e^{\nu_D-\zeta_D}[1-N\beta(1-\beta^2)]\ , \tag{3.28}$$

$$\sigma_0=(N\beta^3/2\pi Gb)e^{\nu_D-\zeta_D}\times\{[1-2N\beta(1-\beta^2)][1-N\beta(1-\beta^2)]\}^{1/2}\ , \quad (3.29)$$

where ν_D,ζ_D are given by (3.17). The first set of brackets is the classical surface density (3.13). σ and σ_0 are illustrated in Figs. 1(c) and 1(d).

The redshift factor (3.10) is simply given by

$$1+z=e^{-\nu_D}=e^{N\beta}\ . \quad (3.30)$$

The largest redshift comes from the center ($\beta=1$), and since we require $V\leq 1$ [cf. (3.22)],

$$1+z_c=e^N\leq e^{3\sqrt{3}/4}\simeq 3.67\ . \quad (3.31)$$

The more extreme limit (3.24) implies $1+z_c\leq 13$.

B. Generalized Schwarzschild disks

These disks are obtained by putting a uniform rod of length $b-a$ at a distance a below the $z=0$ plane along the negative z axis and using Kuzmin's trick. The potential ν is thus [cf. (2.44)]

$$\nu=N\ln\left|\frac{r_a+|z|+a}{r_b+|z|+b}\right|\ ,\quad b\geq a\ , \quad (3.32)$$

where

$$r_a^2=R^2+(a+|z|)^2\ ,\quad r_b^2=R^2+(b+|z|)^2\ . \quad (3.33)$$

The corresponding classical surface mass density of the disk reads

$$\Sigma=\frac{N}{2\pi G}\left[\frac{1}{r_{a0}}-\frac{1}{r_{b0}}\right]\ ,\qquad r_{a0}^2=R^2+a^2\ ,\quad r_{b0}^2=R^2+b^2\ . \quad (3.34)$$

The parameter N is now related to the total mass M of the disk as follows:

$$N=\frac{GM}{b-a}\ . \quad (3.35)$$

We introduce radial parameters similar to β in Kuzmin-Curzon disk:

$$\beta=\frac{b}{(R^2+b^2)^{1/2}}\ ,\quad \alpha=\frac{a}{(R^2+a^2)^{1/2}}\ . \quad (3.36)$$

The square of classical rotational velocity can be written simply

$$v^2=N(\beta-\alpha)\ , \quad (3.37)$$

and the classical angular velocity is thus

$$\omega=[N(\beta-\alpha)]^{1/2}/R\ . \quad (3.38)$$

Relativistic disks of these sorts are described by an additional function ζ [see (2.43)]:

$$\zeta=2N^2\ln\left|\frac{(r_a+r_b)^2-(b-a)^2}{4r_ar_b}\right|\ . \quad (3.39)$$

For

$$N=\frac{GM}{b-a}=\frac{1}{2}\ , \quad (3.40)$$

(3.32) and (3.39) represents Schwarzschild's solution in Weyl's coordinates. Spacetimes with $N\neq\frac{1}{2}$ were analyzed by Zipoy and Voorhees [11]. This family of disks we call generalized Schwarzschild disks.

The potentials in the plane of the disk are

$$\nu_D=N\ln\frac{r_{a0}+a}{r_{b0}+b}\ ,\qquad \zeta_D=2N^2\ln\frac{(r_{a0}+r_{b0})^2-(b-a)^2}{4r_{a0}r_{b0}}\ . \quad (3.41)$$

The energy-momentum tensor components of the disk (2.7) and (2.8) are here given as

$$-\tau_t^t=\sigma=\frac{N}{2\pi G}\left[\frac{1}{r_{a0}}-\frac{1}{r_{b0}}\right][1-N(\beta-\alpha)]e^{\nu_D-\zeta_D} \quad (3.42)$$

and

$$\tau_\phi^\phi=\sigma V^2=\frac{N^2}{2\pi G}\left[\frac{1}{r_{a0}}-\frac{1}{r_{b0}}\right](\beta-\alpha)e^{\nu_D-\zeta_D}\ . \quad (3.43)$$

The velocity squared is therefore

$$V^2=\frac{\tau_\phi^\phi}{-\tau_t^t}=\frac{N(\beta-\alpha)}{1-N(\beta-\alpha)}=\frac{v^2}{1-v^2}\ . \quad (3.44)$$

The maximum value of the function $V(R)$ must be smaller than 1. It is easily seen that the maximum occurs at

$$R^2=b^2\left[\frac{a}{b}\right]^{2/3}\left[1+\left[\frac{a}{b}\right]^{2/3}\right]\ . \quad (3.45)$$

At that point, $V^2\leq 1$ if

$$N\leq\frac{1}{2}\frac{1}{\beta-\alpha}\leq\frac{1}{2}\frac{[1-(a/b)^2]^{1/2}}{[1-(a/b)^{2/3}]^{3/2}}\ . \quad (3.46)$$

The upper bound of N increases from $N=\frac{1}{2}$ for $a/b=0$ to $N=\infty$ for $a/b=1$. For $N<\frac{1}{2}$, $V^2<1$ is always satisfied.

$V^2\leq 1$ is the dominant energy condition. A weak-energy condition results from requiring $-\tau_t^t\geq 0$. As in the Kuzmin-Curzon disk, the weak-energy condition gives an upper limit of N twice as high as compared with the dominant energy condition.

The angular velocity (3.6) reads

$$\Omega=\omega\left[\frac{r_{a0}+a}{r_{b0}+b}\right]^{2N}[1-N(\beta-\alpha)]^{-1/2}\ , \quad (3.47)$$

where $\omega=[N(\beta-\alpha)]^{1/2}/R$ is the classical value; and the specific angular momentum (3.7) now takes the form

$$h/b=(b/a)^N\beta^{-1}(1-\beta^2)^{1/2}[\alpha(1+\beta)/\beta(1+\alpha)]^N\times\{N(\beta-\alpha)/[1-2N(\beta-\alpha)]\}^{1/2}\ . \quad (3.48)$$

Again, it is readily seen that $h/b\propto R^{1/2}$ at $R\rightarrow\infty$, i.e., as in the classical case, but h exhibits more complicated behavior at smaller R (see below).

The surface densities of mass and rest mass are given by the expressions

$$\sigma=[(N/2\pi G)(r_{a0}^{-1}-r_{b0}^{-1})]e^{\nu_D-\zeta_D}[1-N(\beta-\alpha)]\ , \tag{3.49}$$

$$\sigma_0=[(N/2\pi G)(r_{a0}^{-1}-r_{b0}^{-1})]e^{\nu_D-\zeta_D}\times\{[1-2N(\beta-\alpha)][1-N(\beta-\alpha)]^{1/2}\}\ . \tag{3.50}$$

The initial square brackets give the classical surface density (3.34).

For the generalized Schwarzschild disks, the redshift factor (3.10) reads

$$1+z=\left[\frac{b+(b^2+R^2)^{1/2}}{a+(a^2+R^2)^{1/2}}\right]^N . \tag{3.51}$$

The highest values are again for emitters located at the center:

$$1+z_c=\left[\frac{b}{a}\right]^N>1\ . \tag{3.52}$$

The upper limit is restricted by the dominant energy condition, which bounds N by (3.46). For N given by the equality in (3.46), we can rewrite (3.52) in the form $1+z_c=X^{-Y}$, where $X=a/b$:

$$Y=\tfrac{1}{2}(1-X^2)^{1/2}/(1-X^{2/3})^{3/2}\ .$$

This is a monotonically decreasing function of $X\epsilon\langle 0,1\rangle$. Infinite central redshift is achieved for $X=a=0$, while for $X=a/b=1$, $1+z_c=e^{3\sqrt{3}/4}\simeq 3.67$. This corresponds to a massive point at classical distance b below $z=0$, i.e., to the Kuzmin-Curzon disk [cf. (3.31)].

The last result is evident if we realize that the generalized Schwarzschild solutions go over into the Curzon solution for $b\to a$. Indeed, one can easily check that

$$\lim_{b\to a}\left\{[GM/(b-a)]\ln\frac{r_a+|z|+a}{r_b+|z|+b}\right\}=-GM/r_b\ .$$

C. Comparisons and illustrations

The disks may be compared by exhibiting the circular velocities, etc., as functions of the "circumferential" radius $\tilde{R}=Re^{-\nu(R,0)}$. The physical circumference of the circle $R=$const is then given by $2\pi\tilde{R}$ just as for the circle $r=$const in the Schwarzschild spacetime. In Figs. 1, 2, and 3, we give the velocity curves, the curves of the specific angular momentum, the surface mass-energy density, and the surface rest mass density in the dimensionless form V, h/GM, $GM\sigma$, and $GM\sigma_0$ as functions of the dimensionless radius $\tilde{R}/GM$. These were calculated starting from (3.5), (3.7), (3.8), and (3.9). The plots are given for the Kuzmin-Curzon disks [Figs. 1(a)–1(d)], for the Schwarzschild disks with $N=\frac{1}{2}$ [Figs. 2(a)–2(d)], and for the generalized Schwarzschild disks with $N=\frac{1}{4}$ [Figs. 3(a)–3(d)]. In all the plots, the total mass M of the disks is fixed, but several curves are plotted for all three types of disks, corresponding to different values of the parameter b. The smaller b is, the more relativistic the disk is.

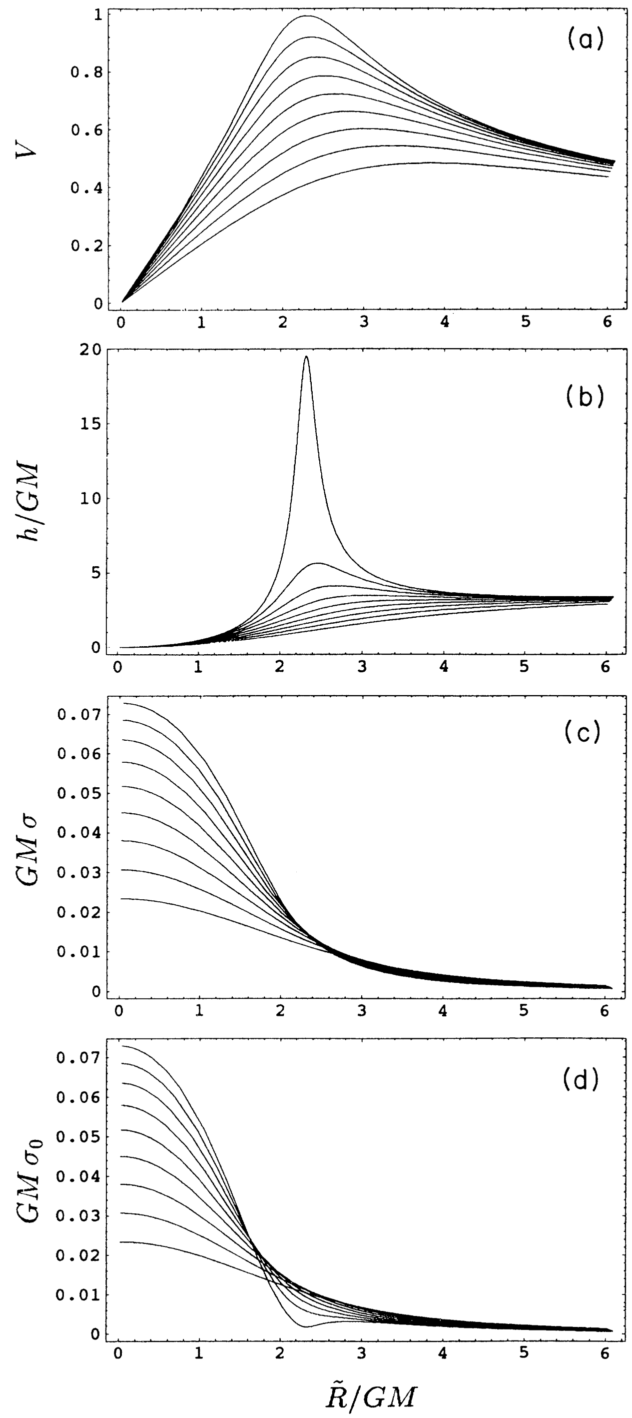

FIG. 1. (a) Velocity curves, (b) the curves of the specific angular momentum, (c) the surface mass-energy density, and (d) the surface rest mass density as functions of the circumferential radius $\tilde{R}$ for nine Kuzmin-Curzon disks corresponding to $GM/b=0.49, 0.59, \ldots, 1.29$. In the highly relativistic disks, as $\tilde{R}$ decreases, V approaches the velocity of light and the specific angular momenta cease to decrease with $\tilde{R}$, but start increasing, indicating thus a relativistic instability. At those radii where $V\to 1$, the rest mass density decreases rapidly with $\tilde{R}$, and it even reaches a local minimum in extreme cases.

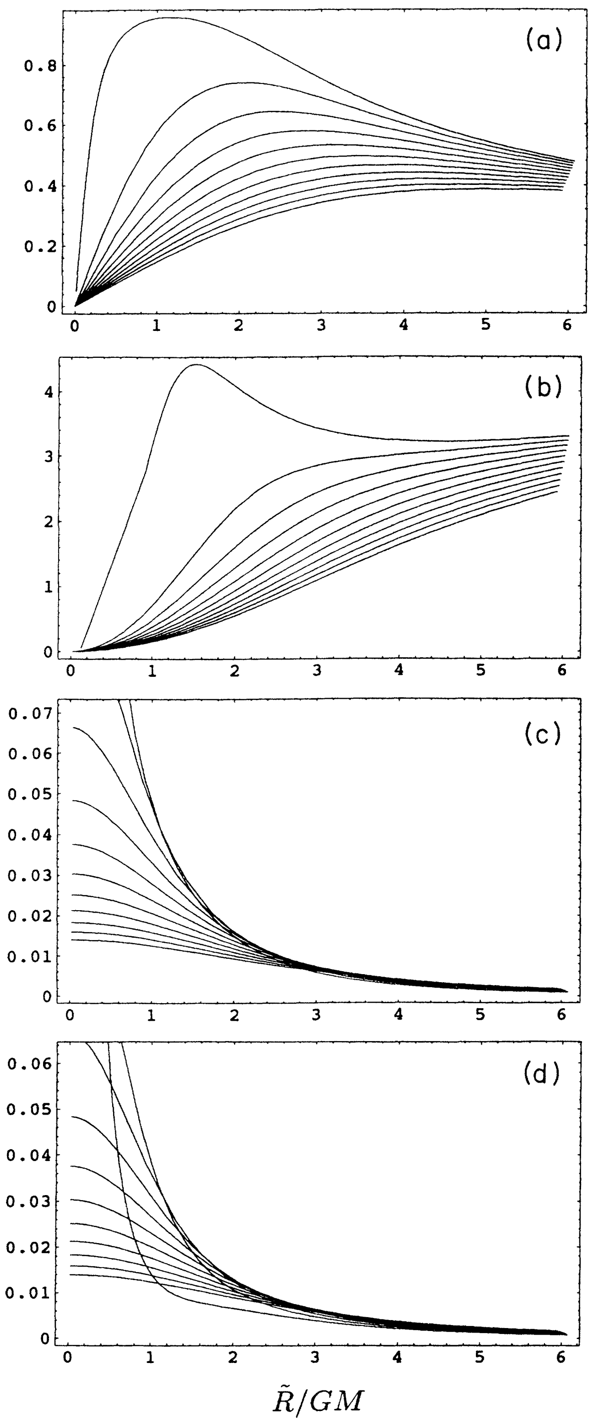

FIG. 2. Same quantities as in Fig. 1 for 11 Schwarzschild disks ($N=\frac{1}{2}$), corresponding to $a/GM=2.01, 1.81, \ldots, 0.01$, or $GM/b=1/4.01, 1/3.81, \ldots, 1/2.01$. In the highly relativistic disk, the relativistic instability associated with the increase of the specific angular momentum again arises, but no local minimum of surface rest mass density occurs.

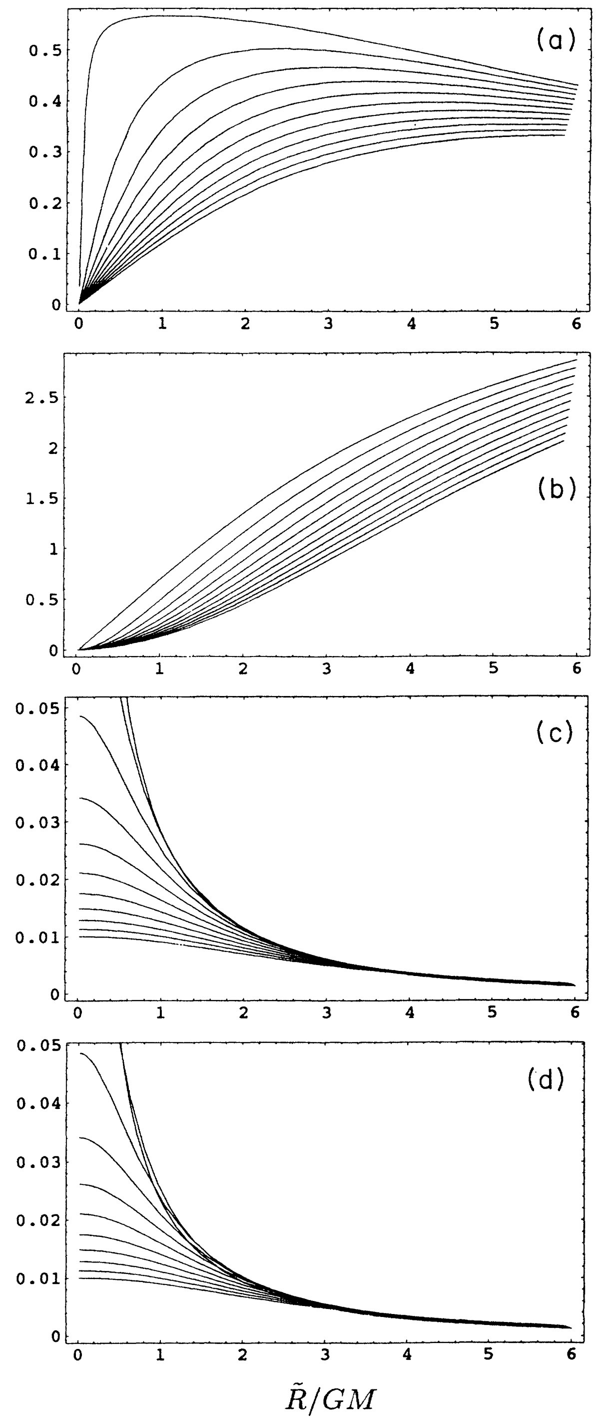

FIG. 3. The same quantities as in Figs. 1 and 2 for 11 generalized Schwarzschild disks ($N=\frac{1}{4}$), corresponding to $a/GM=2.01, 1.81, \ldots, 0.01$, or $GM/b=1/4.01, 1/3.81, \ldots, 1/2.01$. $V_{\max}$ approaches $3^{-1/2}$ in this case. The specific angular momentum always decreases with decreasing $\tilde{R}$, and no local minima in surface rest mass density arise.

In the plots of V and h, the parameter b is getting smaller as one moves from the bottom to the top only at small $\tilde{R}$ — at larger $\tilde{R}$'s, the curves begin to cross.

The maximal relativistic velocities ($V \to 1$) appear at larger $\tilde{R}/GM \approx 2-3$ in the Kuzmin-Curzon disks, i.e., at larger radii than in the generalized Schwarzschild disks. As N decreases, the maximal relativistic velocities occur at smaller $\tilde{R}/GM$. However, V is bounded above by $[N/(1-N)]^{1/2}$, which is less than 1 for $N<\frac{1}{2}$; so it cannot then approach the velocity of light.

This can be shown analytically by using (3.5), (3.41), and (3.45). For $N \le \frac{1}{2}$, the parameter a may approach zero (i.e., the upper end of the rod may approach $R=z=0$, $b \to GM/N$ [cf. (3.35)]) and the maximum velocity is reached close to $\tilde{R}=0$, with its value given by

$$V_{\max}=[N/(1-N)]^{1/2}, \quad N \le \tfrac{1}{2} . \tag{3.53}$$

This effect is clearly exhibited in Fig. 3(a), in which $V_{\max}$ approaches $3^{-1/2} \simeq 0.577$, i.e., the value (3.53) for $N=\frac{1}{4}$. By sending the lower end of the rod to infinity keeping N fixed, one arrives at the infinite-mass constant-velocity disks of Lynden-Bell and Pineault [5]. The corresponding Schwarzschild disk ($N=\frac{1}{2}$) has $V_{\max}=1$ [8].

In the highly relativistic disks, as $\tilde{R}$ decreases, V approaches the velocity of light and the specific angular momenta cease to decrease with $\tilde{R}$, but start increasing. The angular momenta of circular orbits in Schwarzschild spacetime also show such a rise for $r<6m$, which is associated with their relativistic instability. The effect is observed for the three most relativistic Kuzmin-Curzon disks in Fig. 1(b) and for one case of the Schwarzschild disk in Fig. 2(b). No instability of this type arises in generalized Schwarzschild disks with $N=\frac{1}{4}$.

For small a the surface mass densities of the $N \le \frac{1}{2}$ generalized Schwarzschild disks rise rapidly toward the center, behaving as $\tilde{R}^{-1}$ for $a=0$ [see Figs. 2(c), 2(d), 3(c), and 3(d)]. The characteristic radius of the whole mass is always close to b and approaches GM/N as a approaches zero. Nevertheless, these disks have long tails of surface density falling as $\tilde{R}^{-3}$ at large $\tilde{R}$.

An interesting feature may be observed with the highly relativistic Kuzmin-Curzon disks. At those radii where velocities of the streams approach the velocity of light, the *rest* mass density decreases rapidly with $\tilde{R}$, and in extreme cases, it even reaches a local minimum [see Fig. 1(d)]. Such a behavior may be derived analytically, using (3.29) directly.

IV. CONCLUDING REMARKS

Although remarkable progress has been made in finding exact vacuum solutions of Einstein's equations, there are not many explicit solutions with *sources* available which satisfy reasonable physical requirements such as asymptotic flatness and a positive-energy condition. Kuzmin's trick used in classical galactic dynamics has enabled us to construct sources for some known vacuum solutions in the form of counter-rotating disks. The disks are unstable with respect to the formation of (Saturn-type) rings because they lack radial pressure [16]. Such instabilities are suppressed when radial pressures are included; cf. [10]. A truly relativistic instability arises in those disks in which specific angular momentum fails to increase outward at some radius.

Nevertheless, the disks, though extending to infinity, have finite mass and exhibit interesting relativistic properties such as the high velocities of counter-rotating streams and high central redshifts. We are not aware of any other exact solution with a source which is not spherically symmetric that leads to arbitrarily large redshifts. Even in spherical symmetry, one has to conceive quite sophisticated models in order to obtain large redshifts from the center [17]. The primary significance of the disk solutions such as those constructed above lies in the finding of sources, and thus an interpretation, for known vacuum solutions suffering from obscure naked singularities, e.g., Curzon's solution, to name the simplest one [18].

An infinite number of new exact solutions of Einstein's equations can be constructed starting from realistic potentials used to describe flat axisymmetric galaxies, as given recently in closed forms by Evans and de Zeeuw [2]. As special cases, for example, one can find relativistic generalizations of the Mestel and Kalnajs isochrone disks, popular in galactic dynamics. These solutions and their properties will be the subject of another paper [19].

ACKNOWLEDGMENTS

We are much indebted to N. W. Evans for introducing us to the important advance in the theory of axially symmetrical disk potentials embedded within his paper with P. T. de Zeeuw. Had he interacted with us during our work on these disks, he would undoubtedly have been an author too. We also thank C. Pichon for his help.

[1] G. G. Kuzmin, Astron. Zh. **33**, 27 (1956).
[2] N. W. Evans and P. T. de Zeeuw, Mon. Not. R. Astron. Soc. **257**, 152 (1992).
[3] H. Weyl, Ann. Phys. (N.Y.) **54**, 117 (1917). See also independent papers by T. Levi-Civita, Rend. Accad. Lincei **28**, 3 (1919); **28**, 101 (1919). For reviews of this work, see J. L. Synge, *Relativity: The General Theory* (North-Holland, Amsterdam, 1971); D. Kramer, H. Stephani, M. MacCallum, and E. Herlt, *Exact Solutions of Einstein's Field Equations* (Cambridge University Press, Cambridge, England, 1980).
[4] T. Morgan and L. Morgan, Phys. Rev. **183**, 1097 (1969); **188**, 2544(E) (1969). See also T. Morgan and L. Morgan, Phys. Rev. D **2**, 2756 (1970).
[5] D. Lynden-Bell and S. Pineault, Mon. Not. R. Astron. Soc. **185**, 679 (1978). Note that their σ is defined as surface *rest* mass density, and so it is our σ_0.
[6] D. Lynden-Bell and S. Pineault, Mon. Not. R. Astron. Soc. **185**, 695 (1978).
[7] B. B. Godfrey, Gen. Relativ. Gravit. **3**, 3 (1972).

[8] J. P. S. Lemos, Mon. Not. R. Astron. Soc. **230**, 451 (1988).
[9] H. E. J. Curzon, Proc. London Math. Soc. **23**, 477 (1924). See also J. Chazy, Bull. Soc. Math. Paris **52**, 17 (1924), and Ref. [3].
[10] A. Chamorro, R. Gregory, and J. M. Stewart [Proc. R. Soc. London **A413**, 251 (1987)] discuss slow collapse of finite static axisymmetric disks with radial stresses. As an example, they consider the sequence of the "Curzon disks" with the potential which, after a conformal transformation of the (R,z) coordinates, corresponds to a monopole situated at the origin. Their Curzon disks are completely different from our Kuzmin-Curzon disks. Let us also note that self-similar disks with radial stresses were analyzed by J. Lemos, Class. Quantum Grav. **6**, 1219 (1989).
[11] D. M. Zipoy, J. Math. Phys. **7**, 1137 (1966); B. H. Voorhees, Phys. Rev. D **2**, 2119 (1970). For a short summary, see Kramer *et al.*, *Exact Solutions of Einstein's Field Equations* [3], and references therein. Some of these metrics have special names—for example, that corresponding to the line mass density 1 is called the Darmois solution by Kramer *et al.* [cf. G. Darmois, *Me'm. Sci. Mathém.* Fasc. XXV (Gauthier-Villars, Paris, 1927)].
[12] W. Israel and K. A. Khan, Nuovo Cimento **33**, 331 (1964).
[13] W. B. Bonnor and N. S. Swaminarayan, Z. Phys. **177**, 240 (1964).
[14] J. Bičák, C. Hoenselaers, and B. G. Schmidt, Proc. R. Soc. London **A390**, 411 (1983).
[15] S. W. Hawking and G. F. R. Ellis, *The Large Scale Structure of Space-Time* (Cambridge University Press, Cambridge, England, 1973).
[16] A. Toomre, Astrophys. J. **139**, 1217 (1964).
[17] G. S. Bisnovatyi-Kogan and K. S. Thorne, Astrophys. J. **160**, 875 (1970).
[18] For a recent in-depth analysis of the Curzon singularity, see S. M. Scott and P. Szekeres, Gen. Relativ. Gravit. **18**, 571 (1986).
[19] J. Bičák, D. Lynden-Bell, and C. Pichon (unpublished).